In Vitro Characterization of Lactoferrin Aggregation and Amyloid Formation[†]

Melanie R. Nilsson*[,‡,§] and Christopher M. Dobson[§]

Oxford Centre for Molecular Sciences, University of Oxford, South Parks Road, Oxford OX1 3QH, United Kingdom, and Department of Chemistry, University of Cambridge, Lensfield Road, Cambridge CB2 1EW, United Kingdom

Received July 16, 2002; Revised Manuscript Received November 12, 2002

ABSTRACT: Lactoferrin has previously been identified in amyloid deposits in the cornea, seminal vesicles, and brain. We report in this paper a highly amyloidogenic region of lactoferrin (sequence of NAGDVAFV). This region was initially identified by sequence comparison with medin, a 5.5 kDa amyloidogenic fragment derived from lactadherin. Subsequent characterization revealed that this peptide forms amyloid fibrils at pH 7.4 when incubated at 37 °C. Furthermore, although full-length lactoferrin does not by itself form amyloid fibrils, the protein does bind to the peptide fibrils as revealed by an increase in thioflavin T fluorescence and the presence of enlarged fibrils by transmission electron microscopy and polarized light microscopy. The binding of lactoferrin is a selective interaction with the NAGDVAFV fibrils. Lactoferrin does not bind to insulin or lysozyme fibrils, and the NAGDVAFV fibrils do not bind to soluble insulin or lysozyme. The lactoferrin appears to coat the peptide fibril surface to form mixed peptide/protein fibrils, but again there is no evidence for the formation of lactoferrin-only fibrils. This interaction, therefore, seems to involve selective binding rather than conventional seeding of fibril formation. We suggest that such a process could be generally important in the formation of amyloid fibrils *in vivo* since the identification of both full-length protein and protein fragments is common in *ex vivo* amyloid deposits.

Lactoferrin has been identified in amyloid deposits associated with a range of pathological conditions in the seminal vesicles (*1*−*4*), cornea (*5*), and brain (*6*, *7*). Amyloid deposition in seminal vesicles is common among elderly males [21% of men that are more than 75 years of age have detectable deposits (*8*)]. In nonhemodialyzed patients, the deposits contain either lactoferrin or wild-type transthyretin, while in hemodialyzed patients, the deposits contain β-2-microglobulin (*4*). It has also been reported that the protein component of seminal vesicle amyloid has a molecular mass of 14 kDa, although the sequence of the polypeptide that is involved has not been reported. It is therefore possible that this is either an additional amyloidogenic protein or a fragment of one of the above-mentioned proteins (*1*). In the cornea, lactoferrin-containing amyloid deposits have been identified in patients with familial subepithelial corneal amyloidosis (FSCA) (*5*). Some lactoferrin in the deposits appears to be intact, but there are other smaller molecular weight constituents that may be lactoferrin fragments (*5*). This issue, however, is complicated by the fact that lactoferrin from tears (which is the likely source of the protein in this case) is secreted in a variety of forms with different molecular weights. Immunoreactivity to lactoferrin has also been found in pathologic lesions in the brain (*6*, *7*). Lactoferrin immunoreactivity has been identified in senile plaques and neurofibrillary tangles in both Alzheimer's disease and Down's syndrome and in deposits associated with amyotrophic lateral sclerosis and Pick's disease. The role of lactoferrin in amyloid deposition is unclear in all these cases. Lactoferrin may be inherently amyloidogenic or may accumulate as a secondary phenomenon. Lactoferrin has been shown to inhibit the aggregation of some proteins, and it may simply coprecipitate in amyloid deposits (*9*−*11*).

Mature lactoferrin consists of a single 78.3 kDa polypeptide chain of 692 amino acids (Swiss Prot entry P02788). The crystal structure shows two globular domains linked by an α helix (PDB entry 1LFG). Each domain contains one iron (Fe^{3+}) binding site and one site of poly-*N*-acetyllactosaminic glycosylation. The crystal structure of the iron-free form (known as apolactoferrin or iron-depleted lactoferrin) has also been determined and reveals a more open structure (PDB entry 1LFH). Apolactoferrin is secreted in most exocrine fluids, including saliva, bile, pancreatic fluid, tears, and breast milk. Numerous functions have been proposed for lactoferrin, including iron transport and bacteriostasis. In addition, proteolytically derived fragments of lactoferrin have been shown to have antibacterial properties or bind opioid receptors. For reviews on the structure and function of lactoferrin, see refs *12* and *13*.

The primary goal of this research has been to determine if lactoferrin or lactoferrin fragments can form amyloid fibrils *in vitro* and to assess the likely physiological conditions that may promote this process *in vivo*. Apolactoferrin was chosen for these experiments because it is the major secreted form of the protein. In addition, apolactoferrin is known to be more susceptible to denaturation than lactoferrin, and denaturation is often a prelude to aggregation (*14*). Apolactoferrin was partially digested by pepsin to determine if fragments of the

[†] This work was supported by a grant to C.M.D. from the Wellcome Trust.

* To whom correspondence should be addressed: Oxford Centre for Molecular Sciences, Central Chemistry, University of Oxford, South Parks Road, Oxford OX1 3QH, United Kingdom. Phone: 01865 275954. Fax: 01865 275905. E-mail: melanie.nilsson@ocms.ox.ac.uk.

[‡] University of Oxford.

[§] University of Cambridge.

10.1021/bi0204746 CCC: $25.00
Published on Web 12/21/2002

protein may be essential for amyloid formation. Pepsin was selected because this protease is used to generate lactoferricin, a smaller antimicrobial peptide derived from lactoferrin. Lactoferricin is of particular interest because it undergoes an α to β conformational change after cleavage (*15*). In the context of the intact lactoferrin protein, lactoferricin is predominantly α helical, but after cleavage, there is substantial rearrangement into a β sheet conformation. Finally, a synthetic peptide fragment of lactoferrin, the sequence of which is highly identical to that of medin, has been characterized. Medin is a fragment of lactadherin that has been identified in medin amyloid, the most common form of amyloid deposition (*16*).

EXPERIMENTAL PROCEDURES

Sample Preparation

Full-Length Apolactoferrin. Iron-depleted lactoferrin was purchased from Sigma-Aldrich (Fluka Brand 61326, <0.04% Fe). An aqueous 10 mg/mL apolactoferrin stock solution was diluted into 100 mM phosphate buffer (4:1) and incubated as specified in the text to induce aggregation. Additives such as dithiothreitol (DTT),[1] heparin, and NaCl were also included in some samples to observe their effect on aggregation. Sample preparation for the CD experiments is described in the next section.

Pepsin Digests. Pepsin digestions were performed using a previously reported procedure (*17*). In brief, aqueous solutions of apolactoferrin (5 mg/50 μL) and porcine pepsin (Sigma, 3 mg/mL) were prepared and adjusted to pH 3.0 using HCl. Fifty microliters of the pepsin stock was added to the apolactoferrin, and the sample was incubated at 37 °C for 4 h. Reversed phase high-performance liquid chromatography (RP-HPLC) confirmed the presence of a multitude of fragments after digestion.

Peptide Synthesis. A peptide with the amino acid sequence NAGDVAFV (C-terminus amidated and N-terminus free) was synthesized on an Applied Biosystems Pioneer peptide synthesizer using Fmoc chemistry. The peptide was synthesized on a 0.2 mmol scale using 5-{4′-[(Fmoc-amino)-methyl]-3′,5′-dimethoxyphenoxy}valeric acid polystyrene (PAL-PS) resin with 0.22 mequiv substitution to provide C-terminal amidation upon cleavage from the resin. The main solvent for the synthesis was dimethylformamide (DMF), and 20% piperidine in DMF was used for deprotection. Activation was performed *in situ* using HATU, *O*-(7-azabenzotriazol-1-yl)-1,1,3,3-tetramethyluronium hexafluorophosphate, followed by the addition of 8% *N*,*N*-diisopropylethylamine in DMF (v/v). Capping was performed after each coupling step. A cocktail of 3.3% ethanedithiol, 3.3% thioanisole, 3.3% anisole, and 90.1% trifluoroacetic acid was used to cleave the peptide from the resin and remove side chain protecting groups. The crude peptide was purified by RP-HPLC using a C18 preparative column. The identity of the peptide was confirmed by matrix-assisted laser desorption ionization mass spectrometry (MALDI-MS) and amino acid analysis. The molecular masses determined by MALDI-MS were 790.0 and 812.0 g/mol which correspond to the target peptide (calculated, 790.8 g/mol) and the peptide with a sodium ion, respectively. The experimentally determined amino acid composition closely correlates to the calculated values (in parentheses): 25.5% for Ala (25%), 24.4% for Asx (25%), 11.7% for Gly (12.5%), 12.2% for Phe (12.5%), and 26.2% for Val (25.0%). The peptide purity was determined to be greater than 97% by analytical HPLC.

Seeding Experiments. Fibrils of hen egg white lysozyme were prepared by heating 1 mM protein at pH 2.0 to 65 °C for 2 weeks. Fibrils of bovine insulin were prepared by heating 2 mM protein at pH 2.0 to 65 °C for 24 h. The fibrils were separated from unaggregated material using a Centricon and resuspended in pH 7.0 buffer. In the seeding experiments, a 5 μL aliquot of suspended fibrils was added to 50 μL of pH 7.0 buffer (control), an 8 mg/mL apolactoferrin solution in pH 7.0 buffer, a 2 mM insulin solution at pH 2.0, or a 2 mM lysozyme solution at pH 2.0 and incubated at 37 °C (apolactoferrin and insulin) or 65 °C (lysozyme) until an increase in ThT fluorescence was observed.

Circular Dichroism (CD) Experiments

CD experiments were performed on a Jasco J-720 spectrometer. All experiments were performed twice to ensure reproducibility.

Secondary Structure. An aqueous apolactoferrin stock solution of 1 mg/500 μL was prepared and diluted 1 part stock to 39 parts buffer using 100 mM phosphate buffer solutions at pH 4.0, 5.0, 6.0, 7.0, or 8.0. Wavelength spectra were recorded in a 5 mm cuvette at room temperature from 260 to 190 nm using a 1 nm bandwidth, a response time of 1 s, a scan rate of 50 nm/min, and an average of five scans. Measurements were performed both on the day of sample preparation and after incubation for 16 days at 37 °C.

Urea Titrations. Phosphate buffer solutions (100 mM) at pH 4.0, 5.0, 6.0, 7.0, or 8.0 containing between 0 and 8 M urea were prepared. An aqueous apolactoferrin stock solution of 1 mg/500 μL was prepared and diluted 1 part stock to 39 parts buffer. The ellipticity at 222 nm was averaged every second for 60 s using a 1 nm bandwidth.

Temperature Denaturation. An aqueous apolactoferrin stock solution of 1 mg/100 μL was prepared and diluted 2 parts stock to 3 parts buffer using 100 mM phosphate buffers at pH 4.0, 5.0, 6.0, 7.0, or 8.0. The temperature was increased by 1 °C every 2 min using a 0.01 mm water-jacketed cuvette and a Haake thermal bath. The ellipticity at 222 nm was averaged every 20 s from 25 to 80 °C. Wavelength spectra were recorded at 25 °C (before and after heating) and at 80 °C. Spectra were recorded from 250 to 195 nm using a 1 nm bandwidth, a response time of 1 s, a scan rate of 20 nm/min, and an average of five scans. The reversibility of the thermal denaturation was estimated by dividing the difference in the ellipticity at 80 and 25 °C (after heating) by the difference in the ellipticity at 80 and 25 °C (before heating) at 208, 222, and 218 nm. The average value is reported, and error bars show standard deviations (SDs).

Amyloid Detection and Characterization

Thioflavin T Fluorescence. Thioflavin T (7.9 mg) was added to 10 mL of buffer [10 mM phosphate and 150 mM

[1] Abbreviations: CD, circular dichroism; DMF, dimethylformamide; DTT, dithiothreitol; FTIR, Fourier transform infrared spectroscopy; HPLC, high-performance liquid chromatography; MALDI-MS, matrix-assisted laser desorption ionization mass spectrometry; RP, reversed phase; SD, standard deviation; TEM, transmission electron microscopy; ThT, thioflavin T; v/v, volume to volume.

NaCl (pH 7.0)] and filtered through a 0.2 μm filter. The filtrate was diluted into buffer (1 mL to 50 mL) to generate the working solution. The fluorescence intensity of the working solution was measured on a Perkin-Elmer LS50B fluorimeter by excitation at 440 nm (slit width of 5 nm) and emission at 482 nm (slit width of 10 nm). Five microliters of sample was added to 1000 μL of working solution, the mixture stirred for 1 min, and the intensity averaged over 60 s. All data are reported as average values with SD error bars. Dissociation of lactoferrin from the NAGDVAFV fibrils was monitored by two different methods. Lactoferrin was added to a NAGDVAFV fibril/ThT suspension and the fluorescence monitored with time. Additionally, NAGDVAFV/lactoferrin fibrils were purified with a Centricon, added to a ThT solution, and monitored over time.

Fourier Transform Infrared Spectroscopy (FTIR). Samples were solubilized in D_2O, incubated at room temperature for 30 min, lyophilized to remove residual water, and redissolved in D_2O, and the pD was adjusted with DCl and NaOD. FTIR was performed on a Bio-Rad FTS 175C spectrometer using a DTGS detector with 2 cm^{-1} resolution. A dismountable sample cell (CaF_2 plates) was used with a 50 μM Mylar spacer. Sixty-four scans were recorded with a 2 s delay. FTIR was performed in the solid state by drying the sample onto the CaF_2 plate using a gentle stream of nitrogen and desiccation.

Transmission Electron Microscopy (TEM). Samples were placed on a carbon-coated Formvar 200 mesh nickel grid, negatively stained with uranyl acetate, and imaged using a JEOL JEM1010 electron microscope operating at 80 keV.

Congo Red Assays. The specific binding of Congo Red was observed using the spectrophotometric assay (*18*) and by detection of apple green birefringence using our previously reported procedure (*19*).

UV−Visible Spectroscopy. Spectra were recorded on a CARY 3 UV−vis spectrophotometer at 25 °C.

RESULTS AND DISCUSSION

Full-length apolactoferrin is destabilized at low pH but aggregates at high pH. The aggregation of many proteins has been postulated to occur via at least partially unfolded intermediate states (*20*−*24*). Thus, the characterization of the structure and stability of a protein can provide clues about those conditions that may promote aggregation. Apolactoferrin was examined at pH values ranging from 4.0 to 8.0, values that fall within the normal pH range of intracellular and extracellular compartments. The overall shape of the CD spectra (Figure 1) is consistent with previously reported data (*25*). The data indicate that the secondary structure at the different pH values is similar but the protein is slightly less structured at pH 4.0 and 5.0 (Figure 1 inset). The unfolding of the protein was characterized in urea and upon heating (urea titration not shown, thermal denaturation shown in Figure 2A). The midpoint of the thermal transition observed at pH 7.0 (65 °C) is consistent with a previously reported value of 66 °C at pH 7.4 (*14*). In both the urea and thermal denaturation experiments, the protein is less stable at pH 4.0 and 5.0 than at higher pH values. The thermal unfolding was not fully reversible at any pH value; however, at pH 4.0 and 5.0, the recovery of native-like ellipticity was nearly 50%, while between pH 6.0 and 8.0, there was less than 10%

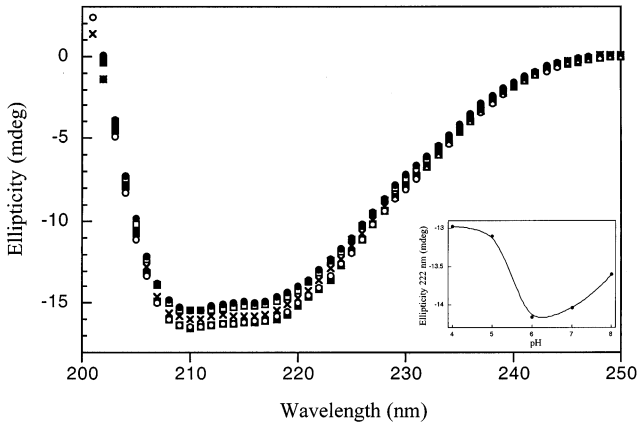

FIGURE 1: CD spectra at 25 °C of apolactoferrin at pH 4.0 (●), 5.0 (□), 6.0 (■), 7.0 (○), and 8.0 (×). The inset is a plot of the ellipticity at 222 nm vs pH.

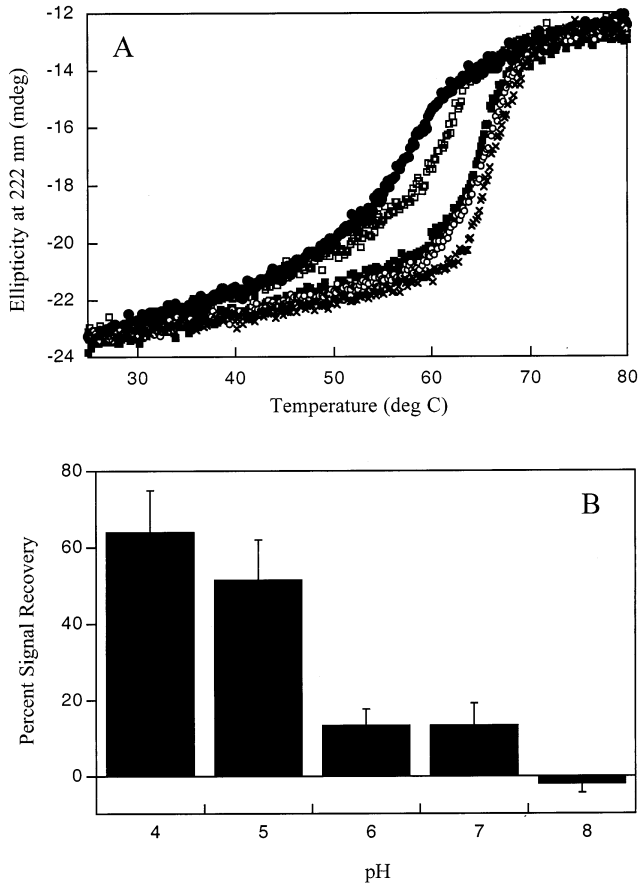

FIGURE 2: (A) Temperature denaturation of apolactoferrin at pH 4.0 (●), 5.0 (□), 6.0 (■), 7.0 (○), and 8.0 (×). (B) The percent signal recovery demonstrates that the extent of protein refolding after thermal denaturation varies with pH.

recovery (Figure 2B). Thus, apolactoferrin is more prone to forming aggregates under thermal stress at pH values at which the native state is the most stable. One explanation for this may be the difference in net charge at different pH values, as electrostatic effects are known to influence the aggregation behavior of proteins.

Full-length apolactoferrin forms amorphous aggregates at elevated temperatures. Apolactoferrin was subjected to a variety of experimental conditions to induce aggregation at 37 °C. No aggregation was observed at pH values between 4.0 and 8.0 even after incubation for 16 days. In fact, the

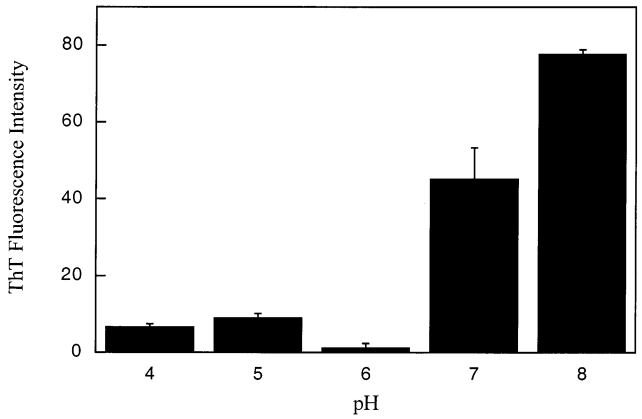

FIGURE 3: Thermal aggregation of apolactoferrin at 65 °C for 1 h characterized by an increase in ThT intensity. Note that no detectable fibrillar structures were observed in these samples by TEM.

CD spectra remained unchanged within experimental error over this time period. This is consistent with the results of Ando et al., who showed that full-length lactoferrin was not observed to form amyloid fibrils between pH 3.5 and 8.0 after incubation for 7 days (50 mM acetate buffer and 100 mM KCl) (*26*). Additional experiments were performed in which 1 mM DTT or 1 mM heparin was added, and again no aggregation was observed. Incubation experiments were also performed at 55, 65, and 80 °C. The samples were examined after incubation for 1 h and 1 day. Very little aggregation was observed by visual inspection or ThT fluorescence for any sample incubated at 55 °C. In contrast, a significant amount of aggregation was observed at 65 and 80 °C, particularly at high pH (Figure 3). These aggregates appeared as white precipitates that gave slightly enhanced fluorescence by ThT. The precipitates were often very sticky, and each precipitate examined by TEM revealed only amorphous deposits without detectable long-range order (i.e., there was no evidence of fibrillar structures). Apolactoferrin was also incubated at 65 °C in the presence of 150 mM NaCl. Significantly more aggregation was observed at low pH upon addition of NaCl, indicating that charge screening may be important for the aggregation of lactoferrin as has previously been noted in other systems (*27*).

Digestion of apolactoferrin with pepsin leads to aggregation and precipitation. The identification of lactoferrin in amyloid deposits *in vivo*, coupled with the information that lactoferrin does not readily form amyloid fibrils *in vitro*, suggests that the nidus for aggregation may be either a fragment of lactoferrin or another amyloidogenic protein. To create lactoferrin fragments, proteolysis was performed using pepsin at pH 3.0. A visible precipitate was observed after pepsin digestion for 4 h at 37 °C. The supernatant and precipitate were examined by TEM and found to contain only amorphous deposits. Experiments were also performed in which the pH was increased from pH 3.0 to 7.4 after digestion for 4 h. Again, no amyloid fibrils were observed in these experiments.

A synthetic peptide derived from lactoferrin is highly amyloidogenic. Of all the known amyloid-forming proteins, lactoferrin is the most similar to lactadherin. Both lactadherin and lactoferrin are glycosylated, multidomain proteins derived from milk and have an established antibiotic function. In addition, A 5.5 kDa internal cleavage product of lactadherin has been found in aortic amyloid deposits *in vivo* and has been named medin (*16*). One segment of medin has been found to be particularly amyloidogenic (*16*), and interestingly, there is a region of lactoferrin that is 63% identical in sequence to this segment of medin (Figure 4). The lactoferrin peptide sequence that spans this region (amino acid sequence NAGDVAFV) consists of residues 539−546 and, in the context of the native protein, acts as part of a connecting loop (residues NAGD) and part of a β sheet structure (residues VAFV). The loop region is partially exposed in the native state. A peptide with the amino acid sequence NAGDVAFV was synthesized and readily forms amyloid fibrils at pH 7.4 as revealed by a significant increase in ThT fluorescence, green birefringence by polarized light microscopy after staining with Congo Red, an increase in β sheet secondary structure content as indicated by FTIR (Figure 5A), and fibrillar deposits observed by TEM (Figure 5B).

```
NPSYARLDKQGNFNAWVAGSYGNDQWLQVDLGSSKEVTGIITQGARNFGSVQFVA
                      *                ** *  * * * **
SCAPGSDPRSNLCALCIGDEQGENKCVPNSNERYYGYTGAFRCLAENAGDVAFVK
```

FIGURE 4: Sequence alignment of medin (top) and residues 493−547 of lactoferrin (bottom). Asterisks mark positions of sequence identity. Medin consists of residues 240−294 of lactadherin. The N-terminal region of medin is often ragged when extracted from *ex vivo* samples, and a synthetic peptide corresponding to this region (underline) was not found to be amyloidogenic. A peptide corresponding to the C-terminal region (bold underline) readily forms fibrils *in vitro* (*16*). The C-terminal region of the lactoferrin sequence (T530−K547) is 39% identical to medin over 18 residues. A lactoferrin-derived peptide (dashed underline), which is 63% identical to the amyloidogenic sequence of medin, is characterized in this work.

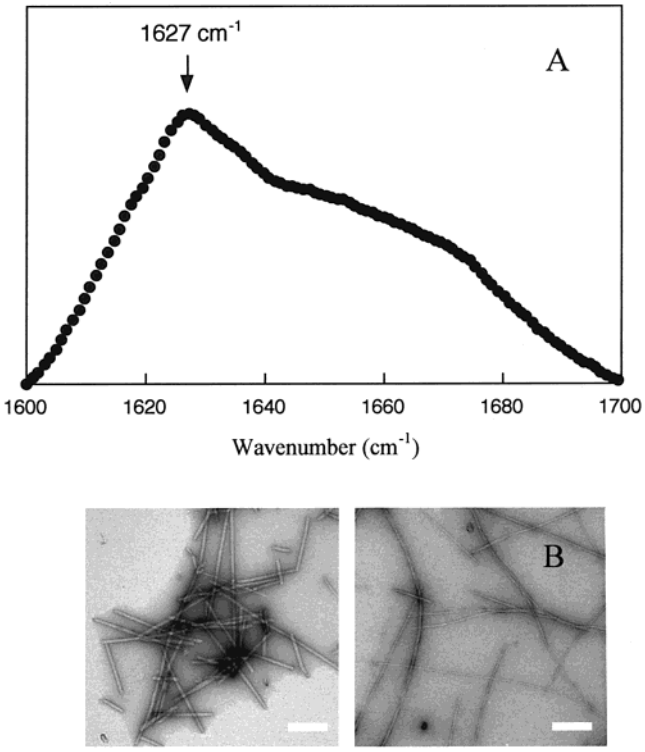

FIGURE 5: (A) FTIR of dried peptide fibrils. The major band is centered near 1627 cm^{-1} and is indicative of β sheet secondary structure. (B) TEM images of peptide fibrils. The scale bars are 200 nm in length.

Seeding experiments demonstrate that a fragment of lactoferrin can induce the full-length protein to aggregate. The results described so far indicate that full-length apo-

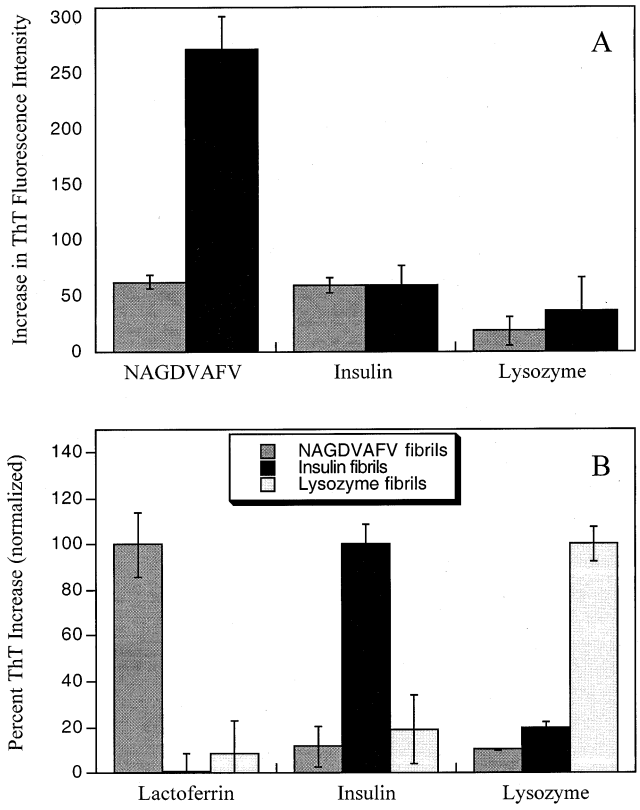

FIGURE 6: Specificity of the interaction between NAGDVAFV fibrils and apolactoferrin. (A) Interaction of different amyloid fibrils with apolactoferrin. Amyloid fibrils composed of either NAGDVAFV, bovine insulin, or hen egg white lysozyme were added to buffer only (gray bars) or an 8 mg/mL solution of apolactoferrin (black bars). (B) The sequence specific interaction between amyloid fibrils and soluble protein is demonstrated by adding different amyloid fibrils to different protein solutions. Three different protein fibril samples (see the inset for the key) were added to freshly prepared protein solutions of apolactoferrin, insulin, or lysozyme. The NAGDVAFV fibrils only lead to an increase in ThT fluorescence intensity when added to apolactoferrin. Likewise, insulin fibrils give rise to an increase in ThT fluorescence when added to insulin and lysozyme fibrils with lysozyme. Thus, each protein fibril leads to the selective aggregation of itself but does not affect the other proteins.

lactoferrin does not readily form amyloid fibrils under a wide range of conditions. It is clear, however, that lactoferrin is present in many amyloid deposits *in vivo*. There are two possible explanations for this apparent discrepancy. First, lactoferrin may be present at these locations and is simply swept into the deposit inadvertently. Second, a fragment of lactoferrin could act as a nidus that leads to the aggregation of the full-length protein. These possibilities were tested by adding preformed fibrils (derived from the lactoferrin peptide NAGDVAFV, hen egg white lysozyme, or bovine insulin) to a solution of apolactoferrin and measuring the change in ThT fluorescence. We postulated that if lactoferrin is simply a protein that adheres to fibrils, we would observe similar changes with all three types of fibrils. In contrast, if the NAGDVAFV peptide fibrils could specifically influence the aggregation of lactoferrin, this would more strongly imply that a lactoferrin fragment acts as a nidus for aggregation *in vivo*. The results of this experiment are shown in Figure 6A. Amyloid fibrils of the NAGDVAFV peptide clearly promote the aggregation of full-length apolactoferrin as revealed by a 4-fold increase in ThT fluorescence after incubation for 1

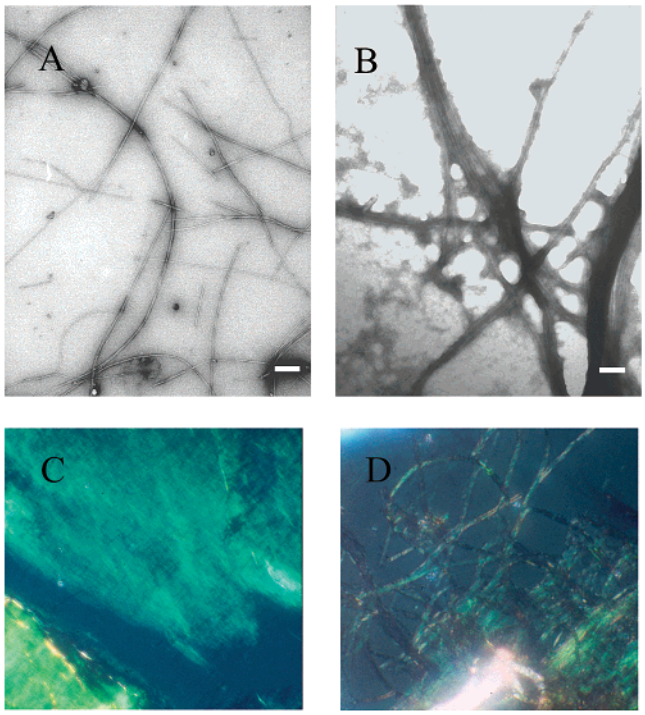

FIGURE 7: Comparison by TEM of (A) NAGDVAFV fibrils and (B) NAGDVAFV fibrils coated with apolactoferrin. The scale bars are 200 nm in length. Congo Red birefringence of (C) NAGDVAFV fibrils and (D) NAGDVAFV fibrils coated with apolactoferrin (40× magnification).

h at 37 °C. This increase in fluorescence is substantially higher than the increase observed upon amorphous aggregation of apolactoferrin due to thermal denaturation (Figure 3). In contrast, addition of amyloid fibrils of lysozyme or insulin does not lead to a substantial increase in ThT fluorescence. Furthermore, the fibrils of the NAGDVAFV peptide interact with lactoferrin but not the unrelated proteins (Figure 6B). Thus, the interaction between apolactoferrin and the NAGDVAFV fibrils appears to be highly specific, suggesting that a peptide fragment may indeed initiate lactoferrin aggregation *in vivo*.

The selective interaction between the NAGDVAFV fibrils and apolactoferrin is not a result of conventional seeding. The apparent seeding of full-length apolactoferrin (a 700-residue protein) by fibrils formed from an eight-residue peptide (NAGDVAFV) is surprising. Thus, further experiments were performed in an effort to understand the nature of this interaction. The fibrils formed upon the addition of NAGDVAFV fibrils to apolactoferrin were examined by TEM and polarized light microscopy. Both techniques revealed fibrils that were significantly larger in diameter than the NAGDVAFV-only fibrils, suggesting that the lactoferrin binds to the peptide fibrils (Figure 7). Therefore, experiments were performed to determine if the lactoferrin binds to the NAGDVAFV fibrils or if the peptide fibrils seed the aggregation of lactoferrin. First, the apolactoferrin samples to which different fibrils were added (Figure 6B) were purified with a Centricon using a 100 kDa cutoff. These conditions allowed full-length apolactoferrin to pass though the membrane, but fibrils were retained. An examination of the filtrates of these solutions by measuring the absorbance at 280 nm revealed 8−10% less apolactoferrin in the sample to which NAGDVAFV fibrils had been added than in the

samples to which lysozyme or insulin fibrils had been added. This suggests that although apolactoferrin is interacting with the NAGDVAFV fibrils, the nature of the interaction is not a conventional seeding process because seeding would be expected to lead to a more substantial reduction in the amount of apolactoferrin in solution.

Fibrils seeding is likely to be more efficient in the presence of more fibril ends. An increased number of fibril ends were produced by freezing the fibrils in liquid nitrogen and thawing at room temperature (this process was repeated three times). The increase in the ThT fluorescence of these fibrils (53 ± 3, $n = 3$) was slightly smaller than the increase in the untreated fibrils (66 ± 3, $n = 3$). This confirms that the interaction of lactoferrin with the NAGDVAFV fibrils does not conform to a classic seeding mechanism. The decrease in ThT fluorescence upon breaking the fibrils to produce more ends may be due to a loss of binding surface area for the apolactoferrin which, evidently, does not have a strong affinity for the fibril ends. The relative ratio of apolactoferrin to peptide in the fibrils was estimated by performing amino acid analysis of purified mixed fibrils and extrapolating the moles of peptide (3.09 nmol) and the moles of apolactoferrin (0.065 nmol) to estimate a relative ratio of 50 mol of peptide to 1 mol of apolactoferrin protein. On the basis of this estimate, the cleavage of the fibrils by freezing and thawing could easily consume a significant amount of the binding surface area of the apolactoferrin, resulting in a decreased ThT fluorescence.

One final experiment was performed to examine the binding interaction of apolactoferrin to the peptide fibrils. The change in ThT fluorescence in the presence of half the concentration of protein or half the concentration of NADVAFV fibrils was examined. If apolactoferrin independently forms fibrils upon addition of NADVAFV fibrils (i.e., conventional seeding), a reduction in the apolactoferrin concentration would be predicted to result in a smaller final ThT fluorescence intensity. In addition, a decrease in the amount of NADVAFV fibrils would be expected to decrease the rate at which the maximum ThT fluorescence intensity is achieved but not alter the final ThT fluorescence intensity. The results of this experiment are shown in Figure 8A. Apolactoferrin itself has no inherent ThT fluorescence, and the ThT fluorescence intensity of the NADVAFV fibrils alone is negligible and is shown at time zero. The next data point represents the time point taken immediately after the addition of NADVAFV fibrils to a solution of apolactoferrin. The final ThT fluorescence intensity is quickly achieved for all samples. Adding half the amount of NADVAFV fibrils leads to a reduction in the final ThT fluorescence intensity by ~50%. Reducing the amount of protein in solution, however, has no effect on the final ThT fluorescence intensity. These results confirm that apolactoferrin is not seeded by the NADVAFV fibrils.

The relative dissociation of apolactoferrin from the peptide fibrils was examined. Two experiments were performed, one to examine the early kinetic events and one to estimate the extent of thermodynamic dissociation. The extent of kinetic dissociation was estimated by adding the peptide fibrils to a solution of ThT and apolactoferrin and measuring the change in fluorescence with time (Figure 8B). There is a slight decrease in fluorescence within the first 500 s, but this decrease parallels the decrease observed upon adding the

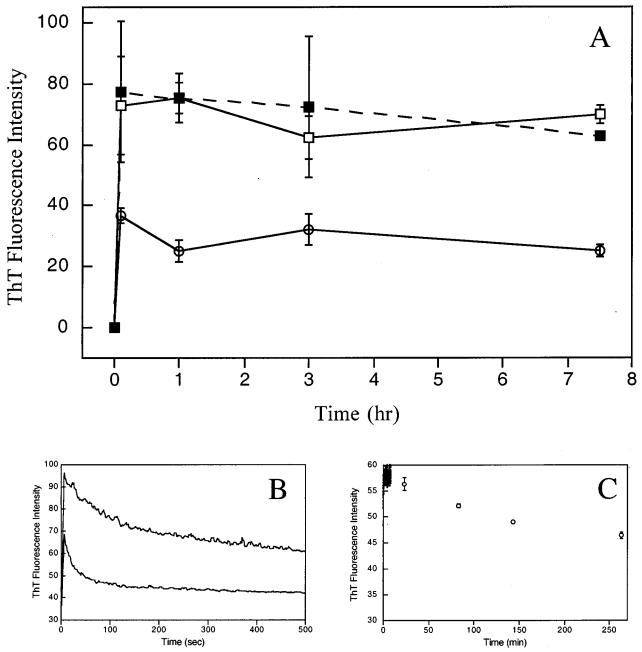

FIGURE 8: (A) NAGDVAFV fibrils selectively bind, but do not seed, full-length apolactoferrin. The addition of NAGDVAFV fibrils (ThT fluorescence shown at time 0) to an 8 mg/mL apolactoferrin solution (no ThT fluorescence) gives rise to an immediate increase in ThT intensity (□). Decreasing the apolactoferrin concentration to 4 mg/mL has no effect on this interaction (■). However, decreasing the amount of seed fibrils in half dramatically decreases the ThT intensity (○). (B) NAGDVAFV fibrils were added to ThT alone (bottom trace) or ThT with lactoferrin (top trace) and monitored with time. The large increase in fluorescence of the lactoferrin binding is apparent. Both samples exhibit a decrease, but this is a result of either optical effects or NAGDVAFV fibril rearrangement upon dilution into sample buffer. (C) Purified NAGDVAFV−apolactoferrin fibrils were diluted 200-fold and examined over time to estimate dissociation. No decrease was observed within the first 500 s, but a decrease in intensity was apparent over the 4 h incubation period. The decrease appears to plateau toward the end of the experiment at a fluorescence intensity that is well above the baseline ThT intensity of 35.

peptide fibrils alone to ThT. Thus, the decrease is either an optical effect or a result of a change in the level of exposure of the peptide fibril surface area upon dilution, but the decrease is not due to significant dissociation of lactoferrin from the peptide fibrils. This experiment, however, was performed with excess apolactoferrin, so an additional experiment was performed on purified peptide−apolactoferrin fibrils. The fibrils were diluted 200-fold into the ThT assay buffer, and monitored for 4 h with constant stirring. There is some degree of dissociation (Figure 8C), but this appears to plateau well above the baseline ThT fluorescence.

CONCLUSIONS

In this work, the structure and thermal stability of apolactoferrin have been examined between pH 4.0 and 8.0. Between pH 4.0 and 5.0, the protein is less structured and less stable than at higher pH values, but the refolding is up to 50% reversible. In contrast, between pH 6.0 and 8.0, the protein is more structured and more stable, but the unfolding leads to aggregation which is not reversible. The addition of NaCl to apolactoferrin solutions resulted in an increased level of aggregation at the lower pH values. This suggests that the charge distribution that exists at high pH values is

more conducive to aggregation than lower pH values, which is consistent with the predicted isoelectric point of pI 8.5 for lactoferrin (pI predicted using ProtParam Tool on the Expasy server).

Although full-length apolactoferrin is prone to aggregation under certain conditions, the conditions that are required to induce aggregation *in vitro* are not close to physiological. Furthermore, the aggregates that are formed are not detectably amyloid-like in nature. Under physiologically relevant conditions (i.e., 37 °C and pH 4.0−8.0), no aggregation was observed even after incubation for 16 days. Similar results were obtained in the presence of either 1 mM DTT or 1 mM heparin. Amyloid formation was only observed by Ando et al. following denaturation, reduction, and blocking of the cysteine residues by iodoacetylation (*26*), conditions which are not likely to be mimicked in a physiological environment. The resistance of native apolactoferrin to forming amyloid fibrils *in vitro* suggests that *in vivo* either a fragment of lactoferrin is present (which contains a lactoferrin epitope and is, therefore, recognized by immunohistochemistry) or the full-length protein is present in amyloid deposits but is itself not able to independently form amyloid fibrils. To this end, we investigated the ability of fragments of apolactoferrin to form amyloid fibrils. Fragments were generated by either pepsin digestion or chemical synthesis. Fragments formed by pepsin digestion formed aggregates, but these aggregates did not contain detectable amyloid fibrils. A synthetic peptide derived from a region whose sequence is highly identical to that of medin (an amyloidogenic fragment of lactadherin) does form amyloid fibrils as indicated by enhanced ThT fluorescence, green birefringence after staining with Congo Red, β sheet secondary structure, and fibrillar morphology. Furthermore, full-length apolactoferrin selectively binds to the peptide fibrils and appears to coat the exposed surface. The nature of the interaction between the peptide fibrils and full-length protein is very specific, unlike proteins such as serum amyloid P (SAP) which have been found in all *ex vivo* amyloid deposits regardless of the sequence of the protein fibril component (*11*).

The peptide fibrils appear to act as a scaffold to which apolactoferrin binds. Apolactoferrin adheres to the peptide fibrils as observed by an increase in fibril width by TEM and polarized light microscopy (Figure 7) and a decrease in ThT upon decreasing the fibril length by freezing and thawing. A dramatic increase in ThT fluorescence intensity is observed upon apolactoferrin binding to the peptide fibrils (Figure 8A), indicating that ThT binds to the mixed peptide−protein fibrils with higher affinity than the peptide-only fibrils. The factors that govern the affinity of ThT binding to peptide and protein fibrils are unknown (*28*), but the increase in fibril surface area and the structural rearrangement of apolactoferrin are possible explanations. The binding of apolactoferrin to the peptide fibrils could occur between the NAGDVAFV sequence of the peptide fibrils and the NAGDVAFV sequence of lactoferrin, which is partially surface exposed in native lactoferrin and would be accessible for binding in a manner analogous to the binding in amyloid fibrils composed of the peptide itself. It is also, of course, possible that the NAGDVAFV fibrils interact with an adjacent part of the protein in a more native-like interaction. Either binding interaction would only require the interaction of a small region of the apolactoferrin protein, and a significant structural rearrangement would not be a prerequisite for binding.

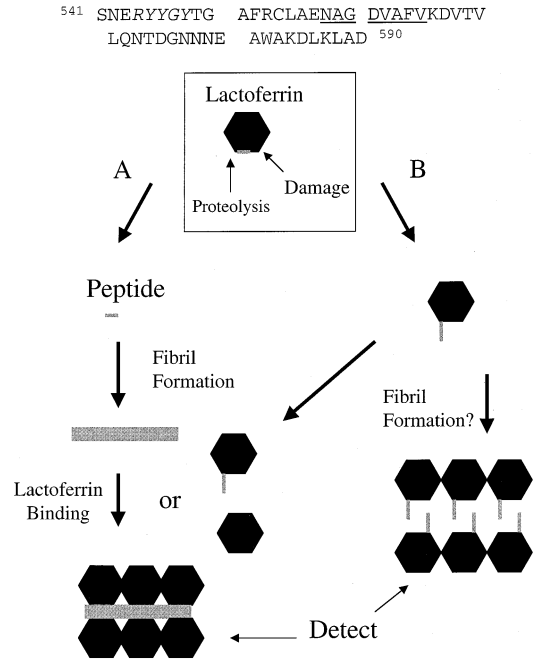

FIGURE 9: Proposed mechanisms of lactoferrin amyloid formation *in vivo*. The sequence of lactoferrin residues 541−590 is shown at the top with the peptide studied in this work underlined. In italics is the sequence of lactoferridoxin B (RYYGY), a known cleavage product of lactoferrin (43). Schematically, lactoferrin is represented as a black hexagon and the amyloidogenic peptide as a gray line. (A) The mechanism characterized in this work could also occur *in vivo*. Proteolysis to generate lactoferridoxin B in addition to aberrant proteolysis and/or hydrolysis could result in the liberation of an amyloidogenic peptide fragment of lactoferrin. The peptide fragment could form fibrils followed by binding of intact lactoferrin. (B) An alternative mechanism may involve proteolysis or hydrolysis that exposes the amyloidogenic amino acid sequence and leads to fibril formation.

These results allow us to propose a possible mechanism for the deposition of lactoferrin in amyloid deposits (Figure 9). First, a highly amyloidogenic region of apolactoferrin becomes exposed, for example, the NAGDVAFV sequence. Cleavage at the N-terminus could be generated by the proteolytic processing of lactoferridoxin B, and cleavage at the C-terminal end could occur via aberrant proteolysis and/or hydrolysis. In support of the latter, it is noteworthy that the sequence that immediately follows NAGDVAFV in lactoferrin is KDVTVLNQNTDGNNN. This sequence contains several side chains that are susceptible to modification. Asparagine attack on the peptide main chain can proceed via a cyclic intermediate, and once ring opening takes place, the backbone can be cleaved (*29*). In addition, there are two aspartic acids in this sequence, residues which are particularly vulnerable to hydrolysis (*30*). The generation of a lactoferrin fragment could lead to rapid fibril formation followed by binding of lactoferrin (Figure 9A). Alternatively, exposure of the amyloidogenic sequence could lead to direct protein assembly (Figure 9B). In both cases, the fibrils would be recognized as lactoferrin by immunohistochemistry and could contain both the full-length protein and fragments thereof. Indeed, the *ex vivo* lactoferrin amyloid deposits that have been examined to date contain evidence of unidentified proteins which may be lactoferrin fragments (*5*) and immu-

nohistochemical evidence that lactoferrin fragments may be present (*2*).

The selective interaction between protein fibrils and a soluble protein with the same sequence or a similar sequence has been demonstrated for many systems that form amyloid fibrils. In fact, the acceleration of aggregation of the native-like protein using fibrils of the same sequence (i.e., seeding) is characteristic of amyloid fibril formation. It is also known that fibrils can seed the aggregation of soluble proteins with a similar sequence, a phenomenon known as cross-seeding. The difference in sequence may be subtle as in the cases of protein damage and mutation (*31*−*33*), or may be slightly more pronounced as is observed in cross-seeding among proteins of different species (*34*), or may even occur between two unrelated proteins that simply share a localized region of sequence similarity (*35*−*37*). The work presented here provides a different example of the interaction that can occur between fibrils and otherwise soluble protein molecules through a selective binding mechanism rather than conventional seeding. This may be the underlying mechanism in other coupled peptide−protein systems in which seeding has been observed and may be particularly relevant in systems for which fibril formation of the full-length protein does not readily occur but peptides derived from the protein rapidly form fibrils *in vitro* (*38*). Furthermore, it is interesting to speculate that such processes may be somewhat general as it is often the case that *ex vivo* amyloid fibrils contain a mixture of peptide fragments and full-length protein (*39*−*42*).

ACKNOWLEDGMENT

MALDI-MS and amino acid analysis was performed by Richard Turner and Peter Sharratt at the Protein and Nucleic Acid Chemistry Facility, Department of Biochemistry, University of Cambridge. Mark Krebs is thanked for technical assistance on the initial thioflavin T experiments and useful discussions. Anne Clark is thanked for advice and assistance on the Congo Red and TEM work.

REFERENCES

1. Cornwell, G. G., III, Westermark, G. T., Pitkanen, P., and Westermark, P. (1992) *J. Pathol. 167*, 297−303.
2. Tsutsumi, Y., Serizawa, A., and Hori, S. (1996) *Pathol. Int. 46*, 491−497.
3. Tsutsumi, Y. (2000) *Int. Congr. Ser. 1195*, 369−375.
4. Suess, K., Moch, H., Epper, R., Koller, A., Durmuller, U., and Mihatsch, M. J. (1998) *Pathologe 19*, 115−119.
5. Klintworth, G. K., Valnickova, Z., Kielar, R. A., Baratz, K. H., Campbell, R. J., and Enghild, J. J. (1997) *Invest. Ophthalmol. Visual Sci. 38*, 2756−2763.
6. Leveugle, B., Spik, G., Perl, D. P., Bouras, C., Fillit, H. M., and Hof, P. R. (1994) *Brain Res. 650*, 20−31.
7. Leveugle, B., Spik, G., Perl, D. P., Bouras, C., Fillit, H. M., and Hof, P. R. (1997) *Exp. Biol. Med. 28*, 119−124.
8. Cornwell, G. G., III, Westermark, G. T., Pitkanen, P., and Westermark, P. (1992) *J. Pathol. 167*, 297−303.
9. Takase, K. (1998) *Nucleic Acids Symp. Ser. 38*, 121−122.
10. Takase, K. (1998) *FEBS Lett. 441*, 271−274.
11. Pepys, M. B., Booth, D. R., Hutchinson, W. L., Gallimore, J. R., Collins, P. M., and Hohenester, E. (1997) *Amyloid 4*, 274−295.
12. Lonnerdal, B., and Iyer, S. (1995) *Annu. Rev. Nutr. 15*, 93−110.
13. Baker, E. N., Anderson, B. F., Baker, H. M., MacGillivray, R. T. A., Moore, S. A., Peterson, N. A., Shewry, S. C., and Tweedie, J. W. (1998) *Adv. Exp. Med. Biol. 443*, 1−14.
14. Hadden, J. M., Bloemendal, M., Haris, P. I., Srai, S. K. S., and Chapman, D. (1994) *Biochim. Biophys. Acta 1205*, 59−67.
15. Hwang, P. M., Zhou, N., Shan, X., Arrowsmith, C. H., and Vogel, H. J. (1998) *Biochemistry 37*, 4288−4298.
16. Häggqvist, B., Näslund, J., Sletten, K., Westermark, G. T., Mucchiano, G., Tjernberg, L. O., Nordstedt, C., Engström, U., and Westermark, P. (1999) *Proc. Natl. Acad. Sci. U.S.A. 96*, 8669−8674.
17. Bellamy, W., Takase, M., Yamauchi, K., Wakabayashi, H., Kawase, K., and Tomita, M. (1992) *Biochim. Biophys. Acta 1121*, 130−136.
18. Klunk, W. E., Pettegrew, J. W., and Abraham, D. J. (1989) *J. Histochem. Cytochem. 37*, 1293−1297.
19. Nilsson, M. R., and Raleigh, D. P. (1999) *J. Mol. Biol. 294*, 1375−1385.
20. Kelly, J. W. (1998) *Curr. Opin. Struct. Biol. 8*, 101−106.
21. Dobson, C. M. (2001) *Philos. Trans. R. Soc. London, Ser. B 356*, 133−145.
22. Khurana, R., Gillespie, J. R., Talapatra, A., Minert, L. J., Ionescu-Zanetti, C., Millett, I., and Fink, A. L. (2001) *Biochemistry 40*, 3525−3535.
23. Mitraki, A., and King, J. (1989) *Bio/Technology 7*, 690−697.
24. Wetzel, R. (1996) *Cell 86*, 699−702.
25. Mazurier, J., Aubert, J.-P., Loucheux-Lefevre, M.-H., and Spik, G. (1976) *FEBS Lett. 66*, 238−242.
26. Ando, Y., Nakamura, M., Kai, H., Katsuragi, S., Terazaki, H., Nozawa, T., Okuda, T., Misumi, S., Matsunaga, N., Hata, K., Tajiri, T., Shoji, S., Yamashita, T., Haroaka, K., Obayashi, K., Matsumoto, K., Ando, M., and Uchino, M. (2002) *Lab. Invest. 82*, 757−766.
27. Chiti, F., Calamai, M., Taddei, N., Stefani, M., Ramponi, G., and Dobson, C. M. (2002) *Proc. Natl. Acad. Sci. U.S.A. 99*, 16419−16426.
28. Levine, H., III (1995) *Amyloid 2*, 1−6.
29. Wright, H. T. (1991) *Crit. Rev. Biochem. Mol. Biol. 26*, 1−52.
30. Inglis, A. S. (1983) *Methods Enzymol. 91*, 324−332.
31. Nilsson, M. R., Driscoll, M., and Raleigh, D. P. (2002) *Protein Sci. 11*, 342−349.
32. Morozova-Roche, L., Zurdo, J., Spencer, A., Noppe, W., Receveur, V., Archer, D. B., Joniau, M., and Dobson, C. M. (2000) *J. Struct. Biol. 130*, 339−351.
33. Wood, S. J., Wypych, J., Steavenson, S., Louis, J.-C., Citron, M., and Biere, A. L. (1999) *J. Biol. Chem. 274*, 19509−19512.
34. Chien, P., and Weissman, J. S. (2001) *Nature 410*, 223−227.
35. Alvarez, A., Opazo, C., Alarcon, R., Garrido, J., and Inestrosa, N. C. (1997) *J. Mol. Biol. 272*, 348−361.
36. Ferrari, G. V. D., Canales, M. A., Shin, I., Weiner, L. M., Silman, I., and Inestrosa, N. C. (2001) *Biochemistry 40*, 10447−10457.
37. Han, H., Weinreb, P. H., and Lansbury, P. T., Jr. (1995) *Chem. Biol. 2*, 163−169.
38. Balbirnie, M., Grothe, R., and Eisenberg, D. S. (2001) *Proc. Natl. Acad. Sci. U.S.A. 98*, 2375−2380.
39. Gustavsson, A., Jahr, H., Tobiassen, R., Jacobson, D. R., Sletten, K., and Westermark, P. (1995) *Lab. Invest. 73*, 703−708.
40. Bellotti, V., Stoppini, M., Mangione, P., Sunde, M., Robinson, C., Asti, L., Brancaccio, D., and Ferri, G. (1998) *Eur. J. Biochem. 258*, 61−67.
41. Kuo, Y. M., Emmerling, M. R., Woods, A. S., Cotter, R. J., and Roher, A. E. (1997) *Biochem. Biophys. Res. Commun. 237*, 188−191.
42. Tagliavini, F., Lievens, P. M., Tranchant, C., Warter, J. M., Mohr, M., Giaccone, G., Perini, F., Rossi, G., Salmona, M., Piccardo, P., Ghetti, B., Beavis, R. C., Bugiani, P. O., Frangione, B., and Prelli, F. (2001) *J. Biol. Chem. 276*, 6009−6015.

BI0204746